Correlated-Photon Experiments Laboratory Manual

Enrique J. Galvez
Colgate University
2008

Index

1. **Introduction**

This manual gives an overview of the laboratory procedures for doing experiments with correlated photons. Our goal is to disseminate a laboratory method that serves to teach the fundamentals of quantum mechanics. The experiments can be set up on an optical breadboard. The experiments that we present here were developed by undergraduates as part of their upper-level laboratory requirement at Colgate University. We later assembled them and offered them as a laboratory component for an undergraduate course on quantum mechanics.

The first section gives useful experimental details for setting up the experiments. The experiments have some inherent challenges. They are not like the standard laser-based laboratories because the light source of correlated photons is too weak. Thus one cannot see the light. This presents an important challenge for the experimenter; alignment of the optics with an auxiliary laser beam (e.g., from a HeNe laser) is indispensable. We got started at Colgate without any prior experience on this type of experiments. We received valuable advice from several researchers. We use our experience as the basis for the recommendations in this manual, and so give our recommendations assuming that the reader is in the same predicament that we were when we started. I will add that in some cases we were stubborn and did not follow the recommendations of the experts, and learned some lessons the hard way. These lessons were valuable, but nonetheless got us in lengthy and sometimes unsuccessful sidetracks. The labs do not require an expert, but they do demand patience. It is hardly a plug-and-play setup. However, once the initial alignment has been completed, the experimental results follow with much ease. Perhaps the most fun part of these experiments is that the results closely follow principles of quantum mechanics that do not have a classical counterpart, such as superposition, entanglement and non-locality. It is a great source of discussion about the fundamentals of quantum mechanics.

While there are a few components that are indispensable: the laser and the detectors, other components can be replaced by equipment that is at hand, such as optical hardware and electronics. This makes the cost of the equipment a variable one. We refer the reader to our recent article that has price lists [1].

The work presented here involved many contributors. Charlie Holbrow got us started by dreaming it up, and convincing us that it could be done. His intuition was incredibly correct: the experiments work! A number of Colgate students helped develop the experiments: Lauren Heilig, Naomi Courtemanche, James Martin, Matt Pysher, Justin Spencer, Kyle Wilson, Kartik Misra, Mehul Malik, Brad Melius, Ushnish Ray and Bryce Gadway. We received valuable advice from researchers in the field: Paul Kwiat, and Anton Zeilinger and co-workers. We were also in close communication with Mark Beck, who does similar experiments at Whitman College. The development of these experiments was funded by the National Science Foundation's Division of Undergraduate Education through grants DUE-9952626 and DUE-0442882.

2. Setting up an Interference Experiment with Correlated Photons

a. Planning Ahead.

There are a few vital equipment components. You need to understand that you need to plan ahead: you need to procure funds and allow time to gather the equipment. Some components take several months to be delivered. In Fig. 1 below we show a view of the layout that we consider to be the most efficient.

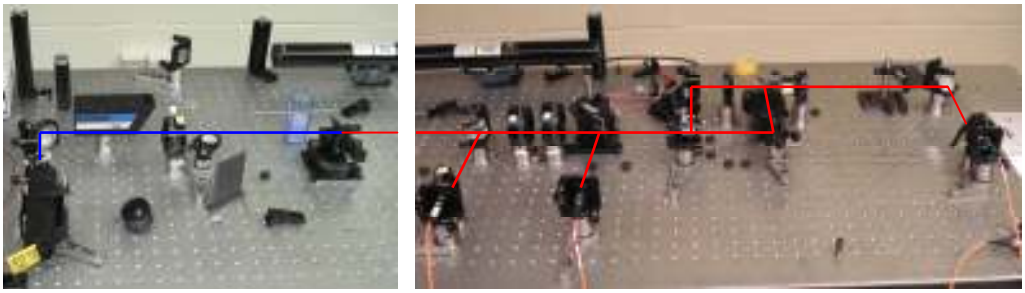

Fig. 1. Layout of the apparatus to do experiments with correlated photons.

Single-photon detectors are a vital component. This is the first item that you should order. We recommend avalanche photo-diodes (APD) operated in the Geiger mode. Unfortunately there is an almost monopoly on this item by EG&G-Canada (owned by Pacer). You need to order two detectors as soon as you can because they take a few months to be delivered. Later we will discuss your options, but let's assume that you acquire an SPCM module, which is what we recommend. This module puts out convenient TTL pulses for every photon that it detects. Its efficiency is in the near infra-red (IR). Figure 2 shows a graph of the published efficiency [2].

If you want to try alternative detectors, you need to look at the single-photon efficiency. Inexpensive avalanche photodiodes can be listed as being very efficient, but for high photon fluxes. The efficiency of photomultipliers in the near-IR is too low.

As can be seen in Fig. 2, the detector has its highest efficiency at 700 nm. As we will see below, the source of light consists of photon pairs generated by spontaneous parametric down-conversion, where the energy of an incoming photon is split into two photons by a non-linear process. For simplicity we do experiments where the two photons have the same energy or wavelength. The ideal source of light is then a pump laser with a wavelength of 350 nm.

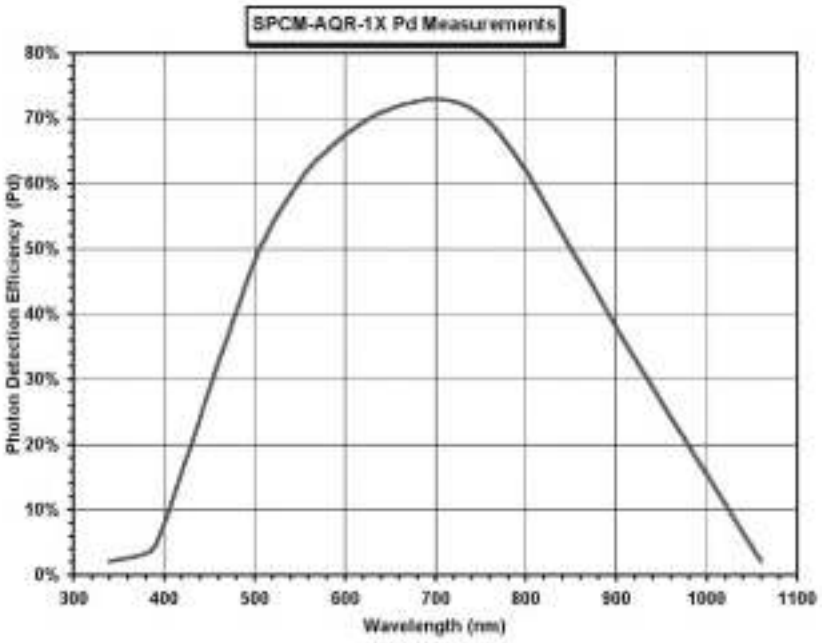

Fig. 2. Typical photon efficiency of a single-photon avalanche photodiode detector from EG&G (Perkin Elmer) [2].

Lasers that operate at this wavelength are expensive argon-ion lasers. Other possibilities are to frequency double a 700-nm laser beam, to then do down-conversion. The best alternative today is the blue-violet GaN diode laser. This type of laser is available at 375 nm, but at low power (few mW), and 405 nm with powers up to 200 mW. When you decide for a laser you also need to know the coherence length of the source, which is determined by the bandwidth of the laser. Anything higher than 1 nm will not be well suited for these experiments.

You will have to know the exact wavelength of the laser, either by a reliable specification by the manufacturer or by making your own measurements. Once you know this wavelength you are ready to order some optics. The next element is the down-conversion crystal. You can order the down-conversion crystal once you know the rough wavelength of your laser. We recommend type-I down-conversion crystals. The main specification is the phase-matching angle. Even this parameter is not critical because one can tilt the crystal if it is not cut at the exact angle.

The next wavelength-dependent optical elements are band-pass filters. These go in front of the detectors. For ordering these one needs to know the exact wavelength of the degenerate down-converted photons. The delivery time is often long (many weeks) depending on the supplier.

For half-wave plates one should purchase zero-order ones. An increasing number of vendors are stocking optics for 405 nm and 808 nm optics, so one can get off-the-shelf items at these or nearby wavelengths. Zero-order wave plates are normally ok if the design wavelength is a few nanometers away from the desired

wavelength.

Next in importance is the electronics. Some can be pricey but readily available. Most items can be built in-house. If you have access to old nuclear physics equipment in "NIM" modules, you may already have all that you need. You need at least three pulse counters (less than 1 MHz is ok), and a module to detect coincidences. We use a "time-to-amplitude" converter that converts the delay between two pulses to a pulse with a height proportional to the delay. A single channel analyzer is used for selecting the pulses from down-converted photon pairs. A multichannel scaler is very useful in helping set the window of the single-channel analyzer. This can also be done by computer control via interface cards and data acquisition software such as Labview.

The remaining optical elements and hardware can be purchased at any time. There is a large variety of vendors and prices. It is useful to make an inventory of the equipment at hand to identify the equipment that is needed.

b. **The Laser**

As mentioned earlier, this is an important component. The detectors that you use have to be reasonably efficient at twice its wavelength. Below is a discussion of the lasers that one can use:

i. GaN lasers (405 nm nominal). These are the best in our view. At ~810 nm the APD detectors are about 60% efficient (see Fig.2), which is quite good. They are also compact, efficient, and do not consume much electrical power. The ones sold as self-contained modules cost about $7k. However, with some expertise in working with diode lasers one can reduce the cost significantly [3]. The bare diodes are still expensive (about $2k), so one has to be careful not to burn the lasers accidentally when handling them. These laser diodes are becoming popular for industrial applications (e.g., future DVD's) so their price is bound to go down. One can do down-conversion experiments with as little as 10 mW. They are now becoming available at powers above 100 mW. However, check the rated bandwidth. High power versions are multimode and could have a large bandwidth and irregular beam profile. There is another option that we can use, which involves diode-laser modules with purely current control (i.e., with no temperature control). These are available fro about $2.5 k.

ii. Argon-ion lasers. These lasers are suitable if we happen to have them around. Otherwise they are quite expensive (e.g., a 350-nm, 200-mW laser is in the $60k-$80k range). There are a number of multi-line argon-ion lasers around, from the days when cw-dye lasers were popular. We have had gotten quite a bit of mileage from one such laser set to its "bluest" line, at 457.9 nm. The efficiency of the detectors at 915.8 nm is still bearable at about 30%. They are also nice because they have high powers (e.g., 200 mW), and have a long coherence length. There are also HeCs lasers, which have an output at 441.6 nm. They are ok for down-conversion as well.

iii. Pulsed lasers. When considering these one should use a high repetition rate laser (e.g. kHz). Low repetition rate lasers (e.g., 10 Hz) have low bandwidth, and large shot-to-shot pulse fluctuations. The rate of accidental coincidences may be too high for low-repetition-rate pulsed lasers. We have not investigated this option thoroughly.

c. **Spontaneous Parametric Down-Conversion**

We have described type-I spontaneous parametric down-conversion in detail before [1]. Briefly, photons of frequency ω_p get transformed into photon pairs (labeled 1 and 2) with frequency ω_1 and ω_2 such that $\omega_p = \omega_1 + \omega_2$. This is not the only condition. The momentum of the light inside the crystal has to be conserved, so the following conditions must be met:

$$n_p\omega_p = n_1\ \omega_1\ \cos\theta_1 + n_2\ \omega_2\ \cos\theta_2 \qquad (1a)$$

and

$$0 = n_1\ \omega_1\ \sin\theta_1 + n_2\ \omega_2\ \sin\theta_2, \qquad (1b)$$

where n_p, n_1 and n_2 are the indices of refraction of the light of frequency ω_p, ω_1 and ω_2, respectively, inside the crystal. The angles θ_1 and θ_2 are the angles formed by the momentum of photons 1 and 2 with the direction of the incident light. When $\omega_1 \neq \omega_2$ down-converted photons 1 leave the crystal forming a cone with half angle θ_1. Photons 2 leave the crystal in the same plane as their partners (1), but forming a cone with half angle θ_2, as shown in Fig. 3.

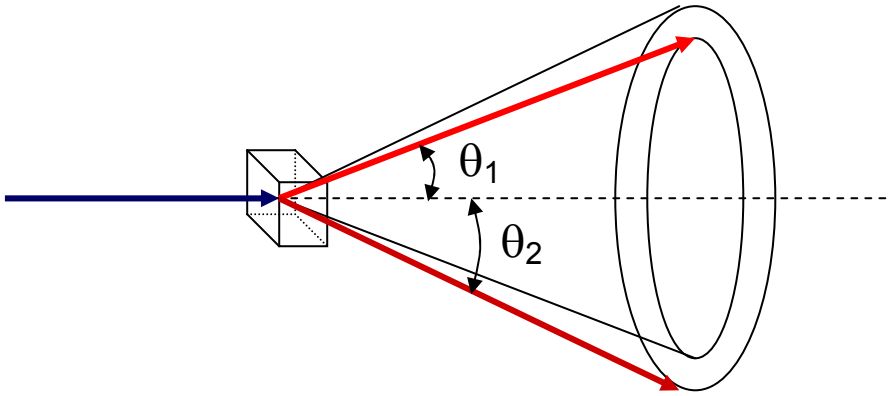

Fig. 3 Schematic of the paths taken by down-converted photons in type-I down conversion.

Thus, down-converted photons come out of the crystal at a range of wavelengths and angles. Thus, past the crystal we do not have any "beams" of down-converted light; down-converted light is all over! In our experiments we select a small subset of the down converted light: those which come out in a horizontal plane, and at the angle where $\omega_1 = \omega_2 = \omega_p/2$. For this degenerate case relation (1a) becomes

$$n_p = n_1\ \cos\theta_1. \qquad (2)$$

This relation specifies that for collinear down-conversion (i.e. θ_m=0) the index of refraction at wavelengths differing by a factor of two must be equal. This is impossible for linear isotropic materials. By using birefringent materials we can

achieve condition (2), via the different indices of refraction of orthogonal linear polarizations. In our case the down-converted photons emerge from the crystal with a polarization perpendicular to that of the pump photons.

The indices of refraction for ordinary and extraordinary rays in beta-barium-borate (BBO), a popular down-converted crystal, are shown in Fig. 4. They are the graphs of the indices as a function of wavelength:

$$n_o(\lambda)= [\ 2.7359 + 0.01878/(\lambda^2 - 0.01822) - 0.01354\ \lambda^2\ ]^{1/2} \qquad (3a)$$

and

$$n_e(\lambda)= [\ 2.3753 + 0.01224/(\lambda^2 - 0.01667) - 0.01516\ \lambda^2\ ]^{1/2}, \qquad (3b)$$

where the wavelength is specified in μm. For example, we measured the wavelength of our laser to be 402.36 nm. At that wavelength the indices of refraction are $n_o = 1.6925$ and $n_e = 1.5675$.

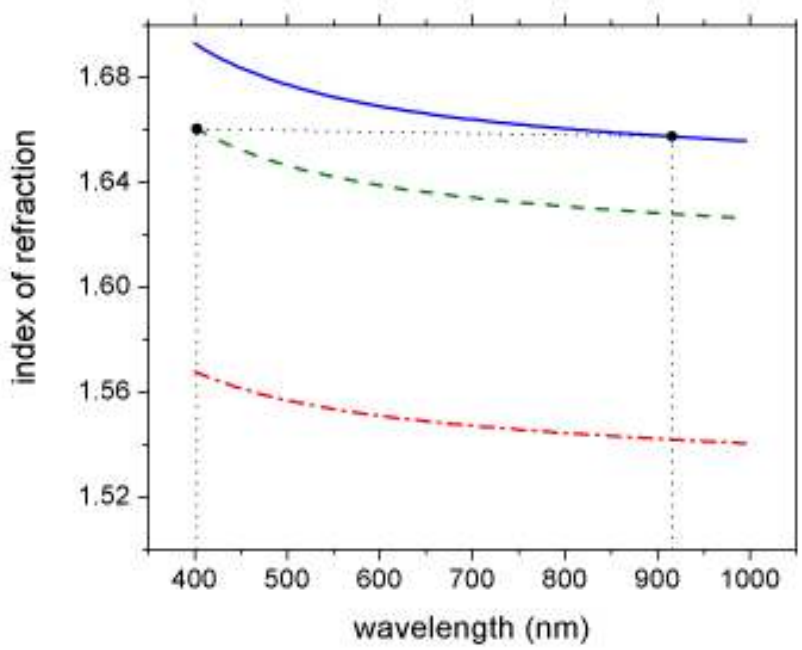

Fig. 4. Index of refraction of BBO for ordinary polarization (blue/solid), full extraordinary (red/dash-dot) and extraordinary at the phase matching angle of 29.0° (green/dash).

In our scheme the down-converted photons are ordinary polarized (i.e., perpendicular to the optic axis of the crystal). The ordinary index of refraction at 804.72 nm is $n_o = 1.6604$. Full extraordinary polarization is when the light polarization is parallel to the optic axis of the crystal. When the polarization of the light forms an angle with the optic axis of the crystal the index of refraction is modified. The relation is normally specified in terms of θ_m, the angle formed by the propagation direction of the light and the optic axis. The index of refraction at an angle θ_m is

$$\tilde{n}_e = [\cos^2\theta_m/n_o^2 + \sin^2\theta_m/n_e^2\ ]^{-1/2}. \qquad (4)$$

By selecting the correct (phase-matching) angle between the optic axis and propagation direction of the pump we can tune the index of refraction to satisfy

Eq. 2. If, for example, we choose to do collinear down-conversion, then we find that $\theta_m = 29.0°$. The green/dashed curve in Fig. 4 corresponds to this phase-matching angle. The phase matching angle changes slowly with the down-conversion angle. For example, if we wished down-conversion at ±3° then the phase matching angle is 29.42°. One also has to remember to use Snell's law when relating the down-conversion angle inside and outside the crystal. We have used crystals not cut exactly to the phase-matching angle, and tilted the crystal by as much as 6°. The crystal may still need a slight fine tuning when we are maximizing down-conversions. This is done once the entire apparatus is setup, by monitoring the coincidences.

We achieve maximum flexibility by mounting the crystal on a rotation stage, as shown in Fig. 5, with its optic axis in a horizontal plane. This requires the pump beam to be horizontally polarized. The resulting down-converted photons are vertically polarized.

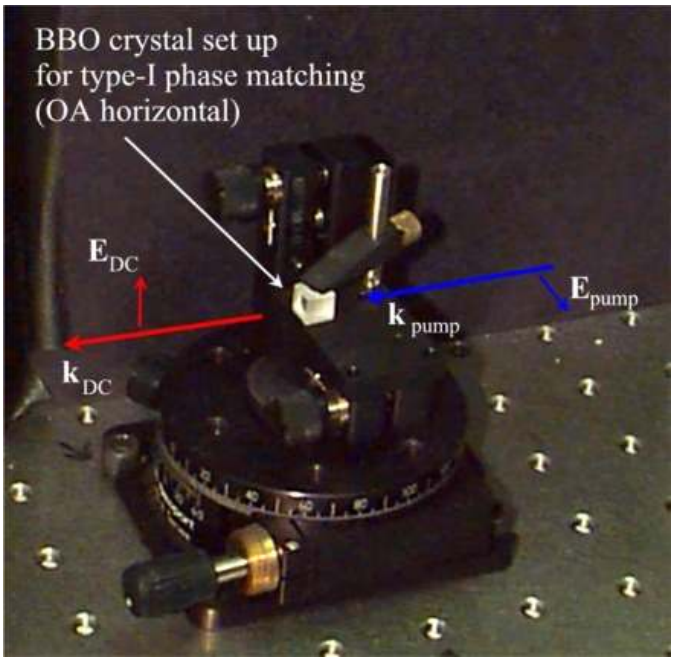

Fig.5. Photo of a BBO crystal as mounted for most flexible adjustments.

In the setup for collinear down conversion we put crossed polarizers before and after the crystal to block the pump beam after the crystal. Absorptive red/IR filters after the crystal may not be suitable because they fluoresce at longer wavelengths creating a large background at the down-conversion wavelengths.

One final note about BBO crystals: they are hygroscopic. We learned this the hard way! When they are left unprotected for extended periods they fog-up. We have found that if the crystals have anti-reflection coatings, they are more resistant to the humidity. We normally cover the crystal mount with a hermetic enclosure with desiccant inside.

d. **Interferometer**

Interference experiments provide an opportunity for students to appreciate quantum mechanics at work via a very dynamic signal. Interference of single photons, although not a proof of the existence of photons, brings the issues of quantum interference to the forefront of the discussion. We have done experiments using many schemes. We find that the simplest one involves collinear down-conversion. It is the easiest to align. Consider the layout shown in Fig. 6. We use a Mach-Zehnder interferometer. This is our favorite interferometer because it is the easiest to understand and align. One can use a Michelson interferometer as well. It has fewer components than the Mach-Zehnder interferometer, but it is harder to adjust to the equal-arm-length condition, an indispensable requirement in these experiments.

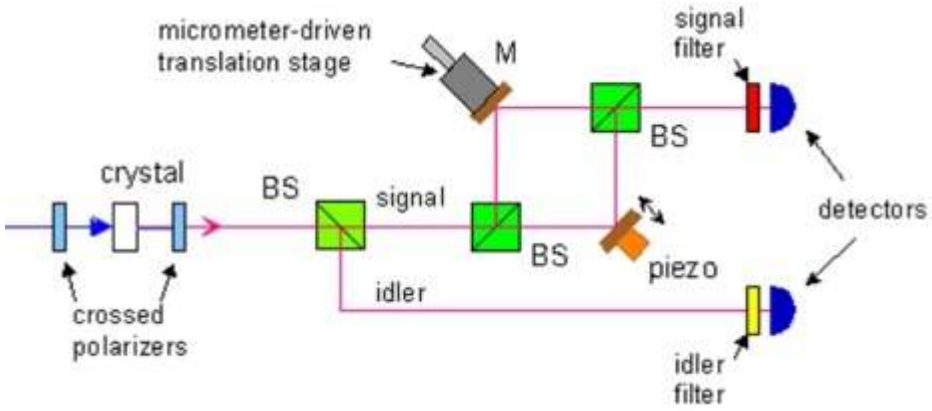

Fig. 6. Simplest layout for interference experiments.

i. **Setting Up the Optics for Collinear Down-Conversion**

In the layout of Fig. 6 one photon, the signal, goes to the interferometer, and the other one, the idler, just goes directly to a detector. We put a beam splitter before the interferometer to split the paths of the two photons. In reality this occurs 50% of the time, but by recording coincidences we discriminate against the cases where they do not split at the beam-splitter.

A vital aspect of setting up the interferometer is to include an alignment laser, such as a HeNe laser. This auxiliary laser beam can be inserted into the path using a mirror that can be reliably positioned after being taken off. We find the "flipper mirror," from New Focus (model 9891, $190), perfectly suited for this.

In order to avoid complications it is best to align all beams with the holes of an optical breadboard. Below we describe our method to do this. We make all of our students working on these projects go through a few-hour training in alignment. We align laser beams parallel to the holes of the breadboard by making it pass through an iris that is translated along the holes of the breadboard.

Suppose that we wish to align a beam after it is reflected off a mirror. The

alignment goes as follows: the beam is first aimed by eye to be parallel to the holes on the breadboard. We put pairs of screws along the same row of holes in two positions: # 1 (near) and # 2 (far). (The screws with the knurled heads from New Focus are very good—we have plenty of these after replacement in other parts with the spring-loaded knobs model TS25) This is shown in "step 1" of Fig. 7.

1. An iris is put in position # 1 with its mount touching the two screws in that position. The iris is then adjusted so that the beam goes through the iris, as shown in "step 2" of Fig. 7.
2. The iris is now put in position # 2, with its mount touching the screws, as in position # 1. If the beam goes through the iris, then it is aligned because from positions # 1 to # 2 the iris has been translated along a line parallel to the holes on the breadboard. If the beam does not go through the iris in position # 2 then the beam must be steered by tilting the mirror until the beam goes through the iris, as shown in "step 3" of Fig. 7.
3. Iterate the previous two steps until the alignment converges.

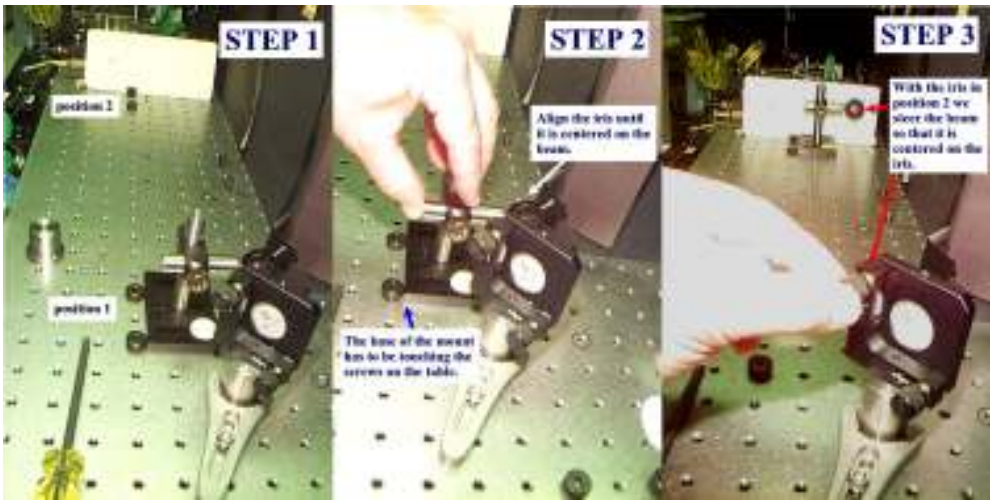

Fig. 7. Method to align beams parallel to the holes on the breadboard.

ii. **Aligning the Interferometer**

We recommend to have all beams no more than two inches above the optical breadboard. This makes the mounts rigid. We have found that the "pedestal" mounts are the best for making compact setups. Interferometers mounted rigidly this way are very stable against vibrations. An optical table is *not* needed. If anything, air currents are the main source of fluctuations in the interference.

The Mach-Zehnder interferometer has two mirrors and two non-polarizing beam splitters. We prefer cube beam splitters. They are easy to mount and align, and they do not produce double reflections. One of the mirrors must be mounted on a translation stage. In our layout of Fig. 6 we have two translation stages one for coarse alignment and another for fine scanning. In one for fine

scanning we put a piezo electric as a spacer (Thorlabs model AE0505D8). It is convenient to have two stages, but one can use one stage for both coarse and fine changes of the path length difference. For sake of stability the interferometer has to be as small as possible. An interferometer with 15-cm sides is small but has enough room for inserting a half-wave plate or polarizer in each arm. For beam-splitter mounts we recommend New Focus 9411 ($309) because it leaves all four beam-splitter ports open.

The alignment should be done by putting the optical elements one by one, as shown in Fig. 8. We first put a beam splitter and align it so that the reflected part of the auxiliary beam is parallel to the rows of holes on the breadboard, as described above. Make sure that the polarization of this beam is either horizontal or vertical. We follow by putting each mirror in sequence, aligning them so that the steered beams are also parallel to the holes of the breadboard. Being rigorous and methodical pays off! Once this is done the beams from the two arms must be intersecting in air. The final step is to put the second beam splitter so that the two beams meet at its beam-splitting surface. We tilt this beam splitter so that the reflected beam is aligned with the holes of the breadboard. Lastly, we adjust the translation stage until the two beams overlap.

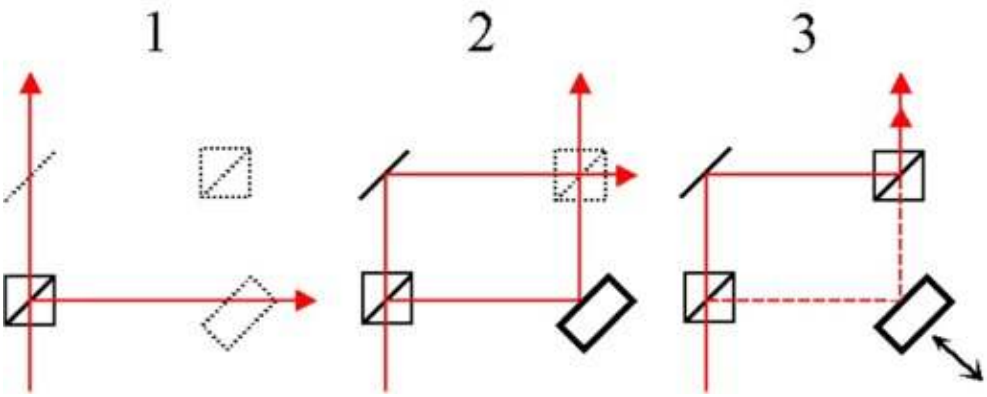

Fig. 8. Schematic of steps for putting together the Mach-Zehnder interferometer. In step 1 the first beam splitter is put. In the second step the two mirrors are installed. Finally the second beam splitter is placed at the intersection of the two beams.

At this point the light from the interferometer can be projected on a screen with the aid of a diverging lens. One must see a very good interference pattern. By tilting the second beam splitter one will see the beams of the two arms overlap perfectly: a bright spot will be seen for constructive interference and no light will be seen for destructive interference. The condition for interference can be changed easily by pulling one of the mirror mounts with a rubber band.

The next step is to align the interferometer so that white-light fringes are seen. The best way to do this is to monitor a spectrum of white light as seen through

the interferometer. The light source should be either a bright white-light LED or a small incandescent bulb (e.g., a 6-V bulb). We use a portable low-resolution spectrometer from Ocean Optics that displays the live spectrum of the light on a computer screen. If the interferometer is aligned systematically as described above, then the length of the arms must be a few microns away from the equal length position. This position will be close enough for the spectrum to show "fringes." Once these are seen we must adjust the translation stage to make the fringes broader (see Fig. 9.), and continue until the entire spectrum oscillates as we touch the stage. This is the equal arm-length position. The interferometer is now aligned.

There are alternate ways to get to the equal arm-length condition. One is to do the previous exercise "by eye." For this we need to observe the white light from the interferometer through a grating. This can be done by either placing a reflection diffraction grating after the interferometer, or by redirecting the light from the interferometer to a transmission grating, as shown in Fig. 10. In both cases we see the white-light fringes through the grating. In the case of Fig. 10 we used a bright white LED as our source of white light.

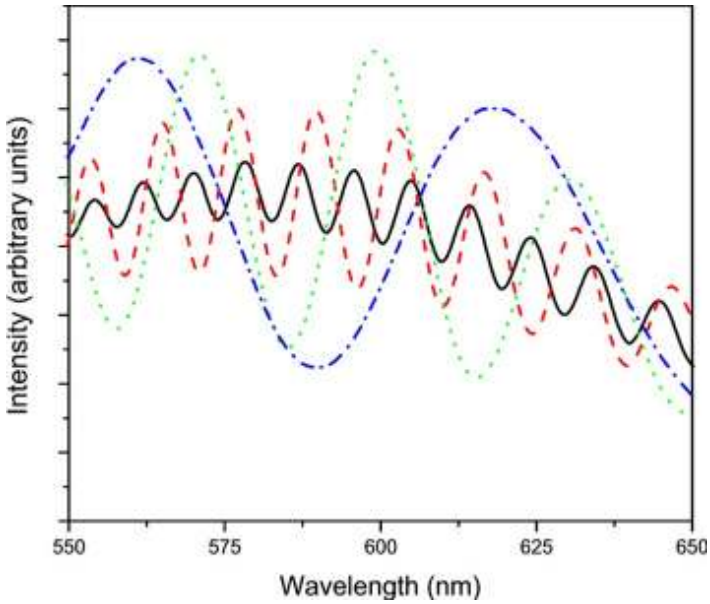

Fig. 9 Spectra of white light as seen through the interferometer. As the difference in length of the arms of the interferometer is decreased the spectrum changes via the sequence of curves shown: black/solid to red/dashed, to green/dot, and to blue/dash-dot.

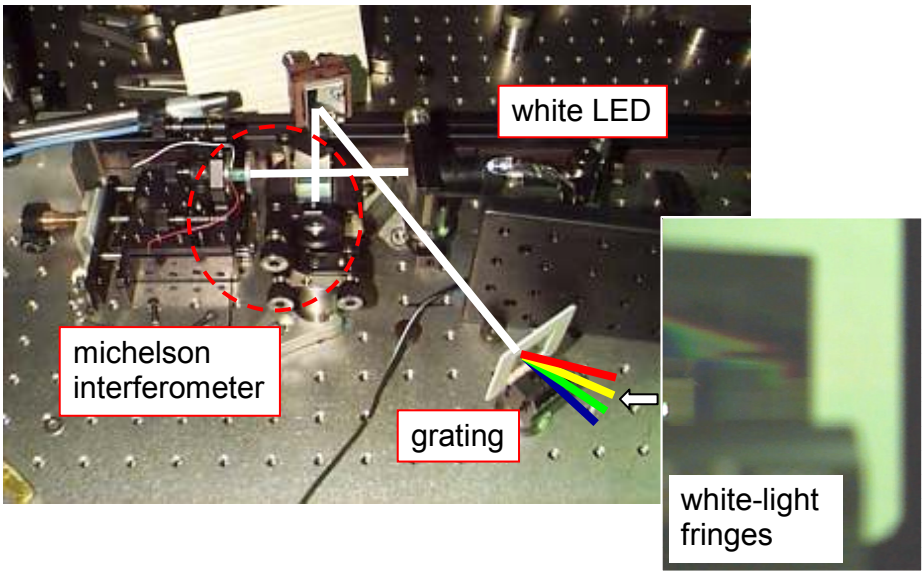

Fig. 10. Setup for observing white-light fringes "by eye." The light from a white LED is sent to an interferometer, and then redirected to a diffraction grating. White-light fringes (i.e., a broken spectrum) is seen through the grating at the equal-arm-length position.

Another way to get to white-light fringes is to send a laser with a poor bandwidth through the interferometer, and observe the fringes with a CCD camera. Diode lasers at threshold have a poor (i.e., large) spectral bandwidth. This results in a small coherence length. Interference fringes with high contrast (visibility) will only be seen very close to the equal-arm-length position. We note that since diode lasers have longitudinal modes in their spectral profile, one will see "revivals" of the interference pattern, with less contrast, at other distances.

iii. The experiment on the quantum eraser entails making the arms of the interferometer distinguishable by the polarization of the light. A polarizer placed after the interferometer erases the distinguishing information. We have used two methods:

1. <u>Using Wave plates.</u>
   The most efficient method is using a zero-order half wave plate to rotate the polarization of the light from being vertical to horizontal. A polarizer placed after the interferometer, with its transmission axis at 45° with the horizontal, projects the two components equally. Because the half wave plate effectively increases the optical path length of one of the arms we need to put another wave plate in the other arm, either aligned vertically or horizontally so that it does not affect the polarization of the light. One could of course change the polarization state in both arms. It could be an interesting student project. The advantage of using wave plates is that we do not lose any light when changing the polarization of the light. The disadvantage is that students then have to understand how wave plates

work.

For mounting wave plates and polarizers we recommend Melles Griot model 07HPR001 ($120). These have an adjustable plate that allows one to align the optics after it has been secured to the mount (it is nice to have axes aligned with 0°!). The gradations in these mounts are in increments of one degree and they are painted on the outside of the mount (so they can be read from the side or top, not the front).

2. Polarizers.
Polarizers are easy to explain quantum mechanically as state projection devices. Thus we can make the lab more understandable if we put a polarizer in each arm, oriented at 45° such that light coming from one arm is polarized at + 45° and the light coming from the other arm is polarized at − 45°. The eraser polarizer could be set to the vertical or horizontal directions. The disadvantage of this method is that near-IR polarizers are neither cheap nor very efficient.

Polarizing cube beam splitters (e.g., New Focus 5812, $300) are good for use outside the interferometer.

e. The detectors.
High efficiency detectors are needed because of a number of reasons. The efficiency in detecting coincidences is the product of the individual efficiencies. Since the source of photon pairs is weak, high efficiencies keep the coincidence rates at a reasonable level. For doing research with single photons one needs high efficiencies. For student-based projects we also need them because low coincidence rates make the experiments difficult. Labs where one cannot get immediate results lose their pedagogical appeal. We want to take a data acquisition scan that lasts minutes, not hours.

When it comes to detectors we are then really stuck with having to use expensive avalanche-photo diode modules. Competition will eventually drive the price of the APD's down. Photomultipliers do not have reasonable efficiencies in the near IR. However, the rise of semiconductor lasers based on intra-cavity quadrupled-frequency YAG, at 266 nm will change the outlook substantially, since photomultipliers are able to detect 532-nm photons with reasonable efficiency.

There are two ways to operate the detectors. One is to use the bare detectors and another one is to couple the light through an optical fiber. We have done both methods at Colgate University, but have less experience with the latter. The detectors are very sensitive to any background illumination. For this reason the experiments are performed in darkened room. If the illumination over the detector goes above a threshold it will burn! Thus, one has to be very methodical about blocking light switches and powering the detectors in a way

that they are not accidentally turned on when the room lights are on.

i. Bare Detectors.

For the case of the bare detectors, we put them in a black-box enclosure with a red/near-IR transmission filter as a window. This allows one to have some background illumination with blue-colored light.

Since the active area of the detectors is 0.25-mm in diameter, we have to use a short-focal-length lens (e.g., 5 cm) to focus the light onto the detector. We need to have the ability to steer the light onto the detector. This can be done by shifting the position of the lens in a transverse plane to the propagation direction. We find the translation mount from ThorLabs (model LM1XY, $128) very convenient.

The detectors have band-pass filters in front of them. For ordinary experiments we use 10 nm filters. Sometimes we use 1-nm filters. The filters determined the bandwidth of the light and thus its coherence length $\ell_c=\lambda^2/\Delta\lambda$, where λ is the wavelength of the down-converted light. For example the coherence length of 804-nm light with a bandwidth of 10 nm is 65 μm.

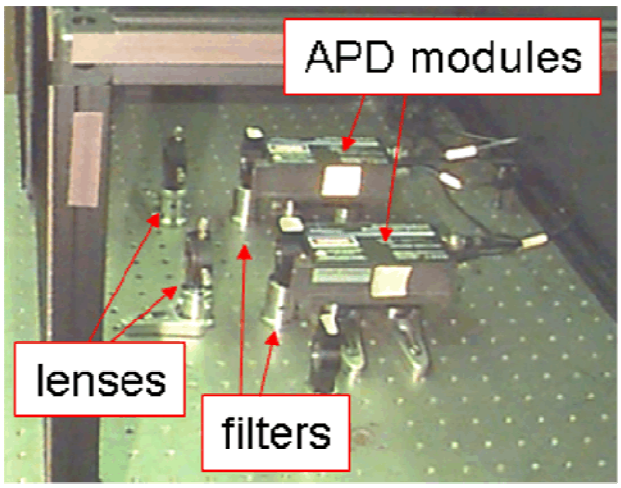

Fig. 11. Picture of the APD modules with the lenses and filters placed in position. In the layout of the picture a large box enclosed both detectors.

We align the detector by first placing the APD so that the auxiliary beam hits it right on. Then we place the lens in a position such that all the light from the beam gets focused on the detector's active area. The final step is to put the filter in front of the detector. When taking data the knobs of the lens translation stage are fine tuned for maximum counts.

ii. Fiber-Coupled Detectors.

The fiber-coupled detectors are more forgiving to the illumination in the room because of the shallow acceptance angle of the fiber. While some

research groups use single-mode fibers, we use 65-μm multimode fiber [4]. At the experiment end of the fiber we use a standard lens coupling. This lens is mounted on a mirror mount. We put a band-pass filter in front of it.

Alignment of the fiber-coupled detectors can be achieved nicely with a fiber-coupled laser: we plug the laser at the end of the fiber (i.e., where the detector would go) and shoot the laser beam out. The tilt of the lens coupler is adjusted so that the beam hits the crystal.

We now use fiber detectors. While each is $4k, a module of four is $10k. It pays to have the extra detectors. Be sure they are all covered when you do experiments. Below we show a picture of the four-detector module. The orange lines are the optical fibers.

f. Electronics.

The electronic signals coming from the detectors go to three destinations, shown in Fig. 12. The first destination is the coincidence module that outputs a pulse every time that a coincidence event is recorded. There are several methods to detect coincidences. We prefer to use the one described below, but there are other options.

In our case it is a time-to-amplitude converter plus single-channel analyzer (TAC/SCA) in Canberra NIM module model 2145. The pulses from the idler detector go to the "start" input of the TAC/SCA. The pulses from the signal detector go through a cable delay (25 ft. coaxial), which introduces a 30-ns time delay. These pulses then go to the "stop" input of the TAC/SCA. The signal and idler pulses also go to stand-alone counters and to the PC interface, which also has counters (National Instruments PCI6601 board and BNC2121 connector box).

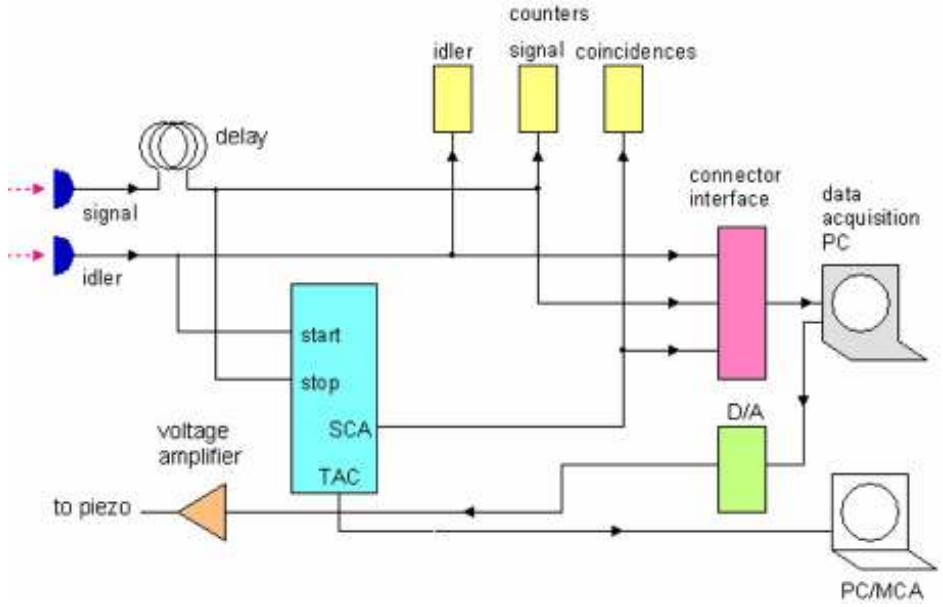

Fig. 12. Schematic of the electronics interface for the experiments. Important blocks: counters, coincidence electronics and data acquisition.

The "SCA" output of the TAC/SCA gives the coincidence events. These pulses go to the stand-alone counter and PC interface. The TAC/SCA has control knobs "T" and "ΔT" that are used to set the coincidence window. That is, we call a coincidence when the idler and the signal pulses are separated by a time between T and T+ΔT. We use a multi-channel scaler to help us set these knobs.

For the interference experiments we have a D/A module to drive the piezo electric that translates the interferometer mirrors. It is a NIM module (Stanford model SR245) that we had. However, it is under utilized, since we only use one of several D/A channels that it has. It could be replaced by a smaller D/A PC board. We amplify the 0-10 V coming out of the D/A interface with a high voltage amplifier (Trek P0515A-1) that we also had at hand. This also has a much less expensive replacement: EMCO model Q02-24 ($80).

For counters we have old NIM module counters. Recently we replaced these with our own inexpensive counters. This is a home-made circuit that uses six-digit decade counter/display (LS7055; few-dollar value). We also have a pulse distribution home-made box. Since pulses have to go to three places, instead of putting cable "T"'s we input each pulse to a circuit that fans out three TTL output pulses. It reduces the mess of wires that results otherwise.

The Data acquisition program in the PC was written in Labview. Figure 13 shows the front panel, which has four graphing screens showing counts as a function of the voltage output for the piezo. The program inputs are starting, ending and increment voltage values and time spent in each step.

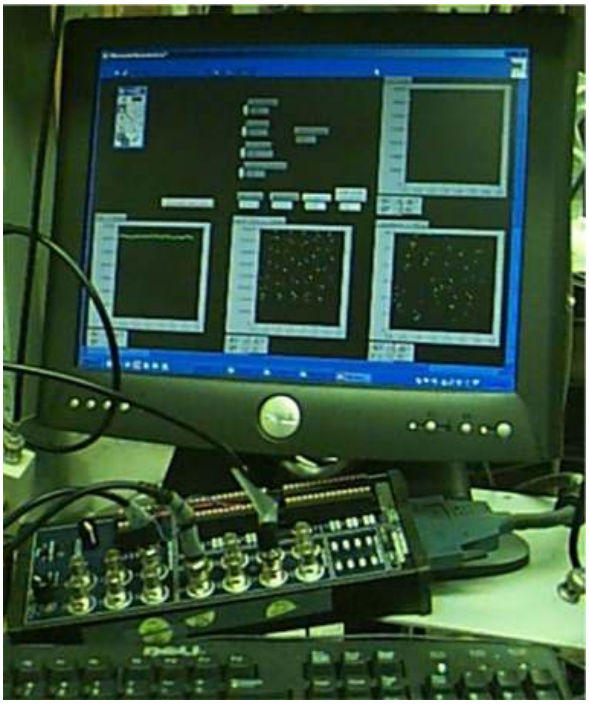

Fig. 13. View of the Labview front panel display.

The figure also shows the cable connector that inputs the signals. The program has the option of a fourth input that we do not use often. The labview counters can also replace the stand-alone counters.

It is useful to test the electronics with a pair of fake signals. For example, set a pulse generator to 50 Hz, putting out pulses like the ones we get from the APD detectors: 4-V, 40 ns long (or less—check yours with a fast oscilloscope). Check that you get the proper readings in the singles counters, coincidences and PC.

g. Taking Data

When all the components are aligned, we turn all the proper equipment and start the search for coincidences. The TAC/SCA knobs should be setup for maximum time window (i.e., T=0 and ΔT=max). With the laser off but detectors on we can see the dark counts from the detectors. These should be a few hundred counts. Beyond a thousand counts is high. We might see some accidental coincidences because the ΔT is all the way up. When you reduce ΔT to a few ns the coincidence counter with the laser off should be zero. The rate of accidental coincidences per second is $N_{acc} = N_i N_s \Delta T$, where N_i and N_s are the singles counts per second for idler and signal, respectively. We do not see significant counts until the singles are in the few hundred-thousand counts.

When we turn the laser on the singles counts should jump up. This reflects the degree of care that you put in setting everything up combined with your own expertise. With our current experience we can put together the setup in a

few hours, and expect coincidences not too long from that. Let's assume that you get some counts in each single counter and no coincidences. Adjust the translating lenses in front of each detector to maximize counts. If the counts go up that is good news. Now adjust the tilt of the down conversion crystal to see those counts go up significantly. Healthy counts are upwards of tens of thousand counts. You can iterate your tuning. If you get nothing, only dark counts, then your crystal may be the problem (we assume that you also searched for obvious mistakes). Check that the optic axis is horizontal and if angled tuned, that it is turned in the correct direction. If you are doing everything right you *should* be getting counts in all three counters by now.

Once you have coincidences then use the multi-channel scaler (MCS) to narrow the window. If you do not have an MCS you can do this by hand: reducing ΔT to a tenth of its maximum value and scanning T by hand. The coincidence peak should be quite prominent over the background of accidentals. Figure 14 shows a graph of counts taken by our MCS. We put as error bars the square root of the number of counts.

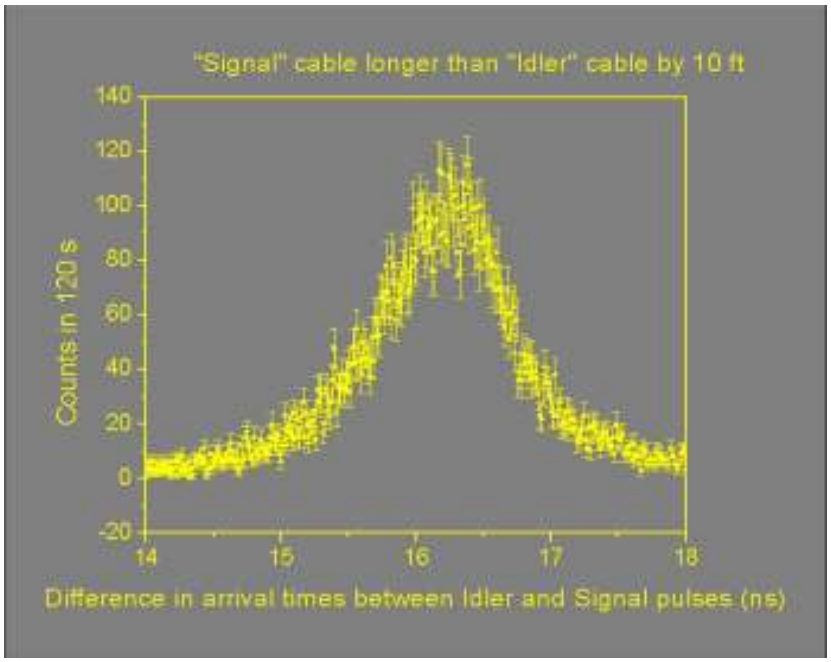

Fig. 14. Graph of the coincidences as a function of the delay between pulses. This is the output of our MCS set to pulse-height analysis.

Verify the properties of down conversion could be part of a student project: monitor coincidences (with small ΔT) as a function of the position of the detectors (vertical or horizontal). One such graph is shown in the Fig. 15.

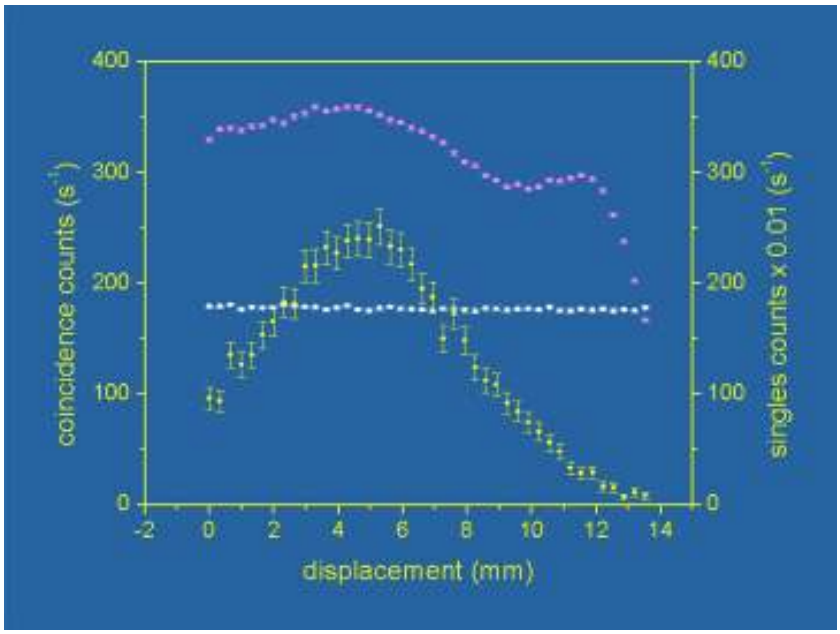

Fig. 15. Graph of counts as a function of the vertical position of one of the detectors. The set of points that change significantly are the coincidences. The other two sets of points are the singles counts from both detectors.

3. Interference Experiments

In this section we make comments on the experiments that we have developed [1].

a. Quantum Eraser

This experiment is interesting because it underscores the way of thinking in quantum mechanics, that quantum interference (i.e., superposition) is possible only when the alternative paths are indistinguishable. This experiment can be explained fully classically, but others cannot. The experiment is useful because it introduces the formalism and the way of thinking.

The idea is that we make the paths of the interferometer by labeling them with the polarization of the light. The down-converted photons are vertically polarized. We label the paths of the interferometer in two ways.

One way involves rotating the polarization of the light in one arm using a half-wave plate. Since the wave plate has an index of refraction higher than air it also effectively lengthens the optical path length of the arm of the interferometer. Since the coherence length can be quite short we must compensate by putting a wave plate of the same material and thickness in the other arm. The wave plate should have its axis aligned with the vertical and horizontal directions so that it does not disturb the polarization of the light going through that arm.

The other method to label the arms uses two polarizers placed in each arm

of the interferometer. The polarizers project the polarization of one arm to the +45° direction (relative to the horizontal), and the polarizer in the other arm projects it into the −45° direction. The only problem is finding reasonable plate polarizers in the near-IR. Any alternative is very expensive ($200-$300), and in addition the polarizer has a significant insertion loss (about 50%).

After the interferometer a polarizer, the "eraser," projects the polarization in an axis at 45° with the two orthogonal polarizations. Below is a graph of a recent experiment that was done as a lab by first-year students. The graph is divided into three sections. In the first section the half-wave plate was oriented vertical, so it did not disturb the polarization and the paths were indistinguishable. As a result we see interference. In the middle section we rotated the wave plate to 45° with the horizontal so that it rotated the polarization of the light by 90° in that arm and thus made the paths distinguishable. In this section the data is flat, showing no interference. In the last section we put a polarizer at 45° with the horizontal after the interferometer that erased the distinguishing information. Notice that the data reproduces the expected probabilities: $P_{indist} = ½ (1 + \cos \delta)$, $P_{dist} = ½$, and $P_{eraser} = ¼ (1 + \cos \delta)$, where δ is the phase due to the difference in path length between the two arms.

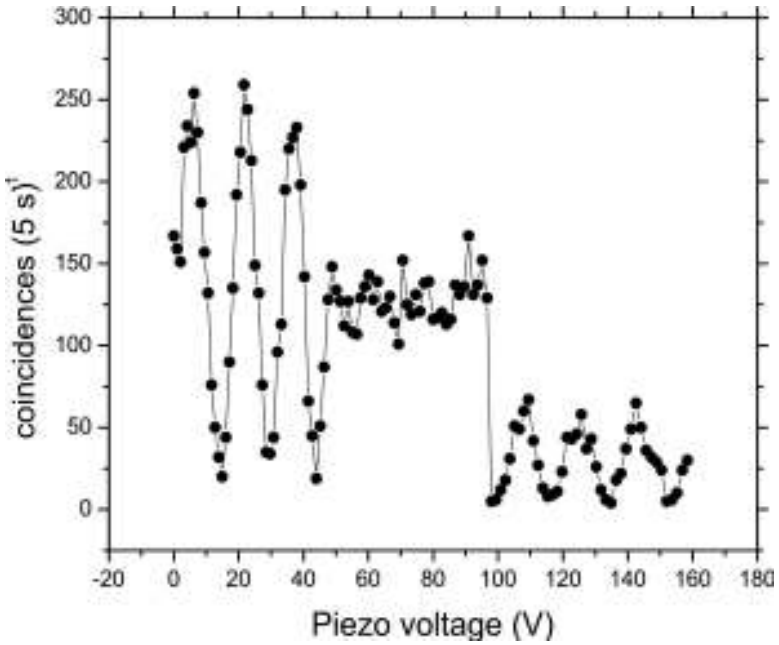

Fig. 16. Data for the quantum eraser (see text).

In the actual lab the optics were all aligned. Students operated the computer, rotated the wave plate and put the eraser-polarizer. They took the data in a disk, analyzed it, and answered a set of questions.

b. Photon wave-packets

In this experiment we start out with the both detectors with 10-nm filters in front of them. When we scan the piezo we see fringes. We then stepwise increase the path length by a discrete amount. After this step a scan shows fringes with reduced visibility. We continue stepping and scanning until the path length is greater than the coherence length. At that point the data shows no interference. The argument here is that the filters specify the bandwidth of the light. If we think of the photons as wave packets their spatial extent is indeed the coherence length. When the arm lengths differ by more than the coherence length the paths become distinguishable because the photon taking the shorter path will arrive distinguishably earlier than if it took the longer path.

We continue by putting a filter with a narrower bandwidth. This increases the coherence length of the light. When this new coherence length is larger than the arm length difference the paths become indistinguishable again and interference is recovered. Figure 17 shows graphs of the data taken by students in the quantum mechanics class offered in 2005. The data shows a progression of curves as the length of one of the arms is stepped. When the data with 10-nm filters was flat we changed the filter in the *idler* to 1 nm. The fringes reappeared (black continuous trace).

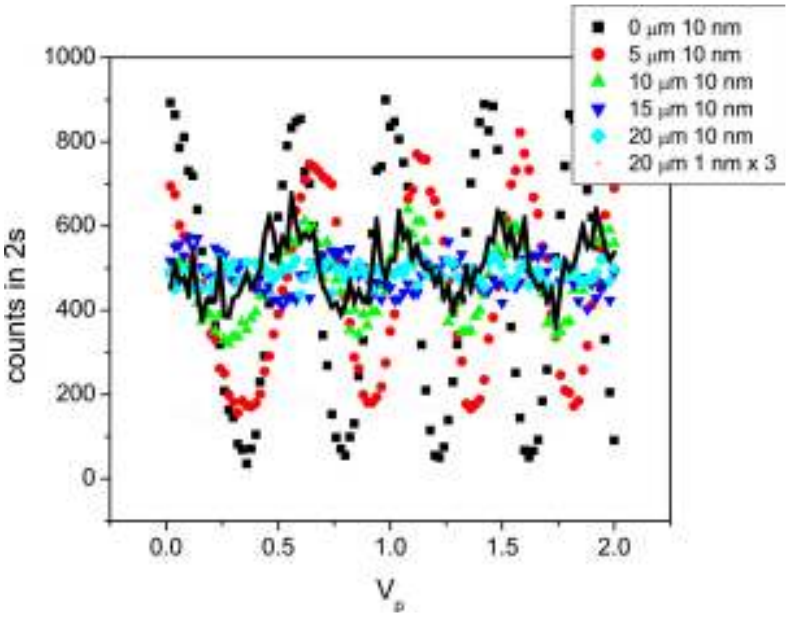

Fig. 17. Data for investigating the effect of the coherence length of the light.

The Biphoton

This experiment cannot be fully explained classically. It is very easy to align because both photons go through the interferometer. That is, we do not have a beam splitter before the interferometer. Instead we have one after the interferometer, as shown in Fig. 18. The beam splitter redirects light onto a second detector

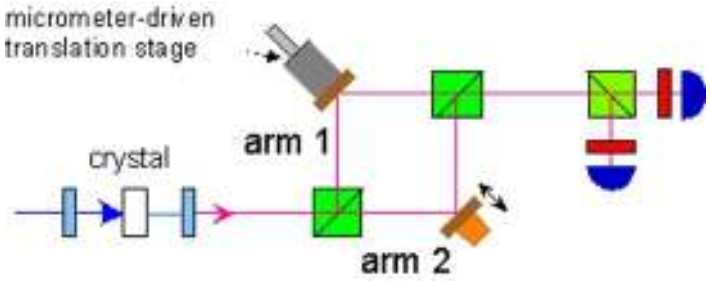

Fig. 18. Setup for the experiments on the biphoton.

The interesting aspect of the data is that the shape of the interference pattern changes with changes in the arm-length difference.

4. **Entanglement**

We produce polarization-entangled states using the method of Kwiat et al. [5]. It consists of two thin type-I down-conversion crystals rotated 90°, as shown in Fig. 19. The input polarization is rotated by a half-wave plate so that half of the light is vertically polarized and the other half is horizontally polarized. The horizontally polarized light produces down-conversion with the first crystal and the vertically polarized pump does it with the second crystal. This produces a set of thinly displaced cones of down converted light at the degenerate wavelength.

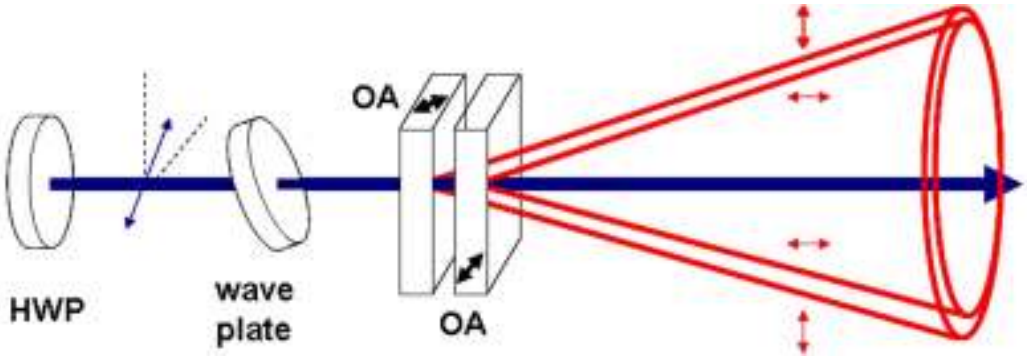

Fig. 19. Method of producing entangled states.

If the crystals are thin (0.1-1 mm) and their separation is nearly zero, then the cones overlap in such a way that one cannot distinguish which crystal light comes from (by means other than polarization). This puts the down converted light in the entangled state

$$|\psi\rangle = 2^{-1/2} \left(|H\rangle_1 |H\rangle_2 + e^{i\phi} |V\rangle_1 |V\rangle_2 \right). \quad (5)$$

The phase ϕ is due to the birefringence of the crystals. This is because waves of different polarizations travel at different speeds inside the crystals. We adjust ϕ to be zero using a wave plate or a birefringent crystal [3]. We use a 1-mm thick multiple-order wave plate that we had at hand, designed for a different wavelength. The axis of the wave plate must be horizontal or vertical. We then tilt

the wave-plate along one a vertical axis to check the tuning.

There are two considerations to make when looking for down conversions of this type. First we need to worry about having the pairs of non-collinear photons at a shallow angle, such as 3°. The smaller the angle the better overlap of the two cones. The degree of overlap determines the purity of the entangled state. The second adjustment involves the tilting of the wave-plate to make ϕ=0.

Doing non-collinear down-conversion presents a considerable challenge. Since we cannot see the light we need to calculate where the beams should be a few tens of centimeters down stream and put the detectors in those locations. It is also important to block the pump beam after the crystal. When in this stage of the alignment set the pump beam to horizontal or vertical polarization so that you do not have to worry about entanglement. You then adjust the detectors to maximize counts in the detectors.

The down-conversion crystals have to be custom-ordered. They can be ordered cemented or placed back-to-back in a dedicated housing. The vendor that we consulted (Cleveland Crystals) recommended against having the two crystals cemented so we had them mounted back to back. They mounted one pair and we mounted the other pair ourselves. We put a thin spacer in between the two so that the surfaces did not touch. All surfaces were coated with anti-reflection coating. You should mount the down conversion crystal pair on a flexible mount. We put first mount the crystal housing on a rotation stage and mount the rotation stage on a mount that can be tilted (we use New Focus' "Opticlaw model 9854, $209). Once we get coincidences we tilt the crystal along the proper axis (vertical axis if the pump beam is horizontal) to maximize coincidences. We then rotate the polarization of the pump beam to the orthogonal polarization and tilt the crystals along the corresponding axis for maximum coincidences.

Rotate the polarization of the pump beam so that it forms 45° with the horizontal and put polarizers in front of the detectors. By now the counts in both polarizations should be nearly equal. If the counts are not equal you may want to adjust the plane of polarization of the pump beam.

The next alignment uses the quantum correlations between the entangled states. When ϕ=0 the state is:

$$|\psi\rangle = 2^{-1/2} \left(|H\rangle_1 |H\rangle_2 + |V\rangle_1 |V\rangle_2 \right). \quad (6)$$

The beauty of entanglement is to realize that this is a true superposition state. That is, that the light is in both states of parallel polarization until a measurement is made. The state above has the nice property that when transformed into another coordinate axis the photons are still in a superposition of parallel polarizations [6]. For example, if we pick the diagonal and anti-diagonal basis (D,A) (e.g., +45° and −45°, respectively) the state becomes:

$$|\psi\rangle = 2^{-1/2} \left(|D\rangle_1 |D\rangle_2 + |A\rangle_1 |A\rangle_2 \right). \quad (7)$$

That is, if we put a polarizer at +45° then we should get no coincidences if the

polarizer in front of the other detector is at −45°. Conversely, if for example $\phi=\pi$:

$$|\psi> = 2^{-1/2} (|H>_1 |H>_2 - |V>_1 |V>_2), \quad (8)$$

then the state transforms to [6]

$$|\psi> = 2^{-1/2} (|D>_1 |A>_2 + |A>_1 |D>_2); \quad (9)$$

in the diagonal basis the photons have orthogonal polarizations! Figure 20 shows scans of the angle of polarizer 2 for fixed positions of the orientation of polarizer 1. In this case the pair was in the state given by Eq. (8). Thus one can set $\theta_1=\pi/4$ and tune the state by repeating these scans of θ_2 until the data show the proper correlations [i.e. minima at $\theta_2=45°$ for the state of Eq. (6)].

These correlations give an appreciation for the algebra of superposition. Of course, the ultimate test is the Bell test [7]. However, the Bell test is less dynamic because it comes down to computing a number. A more appealing test of non-locality is a scan of the correlations for an entangled state and another one for a mixed state. A mixed state is obtained by setting pump polarization horizontal for half the time of each data point and vertical for the other half of the time in each data point. In this case, at any given time the light is either horizontally polarized or vertically polarized. One can easily show that when $\theta_1=0$, $\pi/4$ and $\pi/2$ the detection probability of the mixed state is $P_{mixed} = ½ \cos^2 \theta_2$, $P_{mixed} = ¼$ and $P_{mixed} = ½ \sin^2 \theta_2$, respectively. This is in contrast with the entanglement of Eq. (5) where it is $P_{pure} = ½ \cos^2(\theta_1-\theta_2)$.

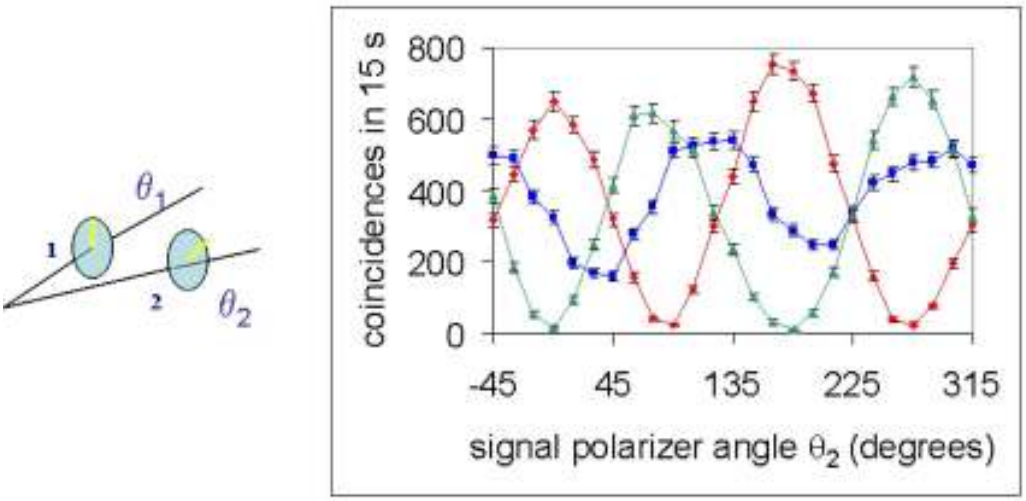

Fig. 20. Measurements of the photon correlations when the pairs are in the state given by Eq. (5). In the data sets are for $\theta_1 = 0$ (red) with $\theta_1 = \pi/4$ (green) and $\theta_1 = \pi/2$ (blue).

For additional information check our website:
http://departments.colgate.edu/physics/pql.htm

References

1. E. J. Galvez, C. H. Holbrow, M. J. Pysher, J. W. Martin, N. Courtemanche, L. Heilig, and J. Spencer," Am. J. Phys. **73**, 127 (2005).
2. Single Photon Counting Module SPCM-AQR Series, Perkin Elmer Optoelectronics product report (Perkin Elmer,2001).
3. D. Dehlinger and M. W. Mitchell, Am. J. Phys. **70**, 898 (2002)
4. J. J. Thorn, M. S. Neel, V. W. Donato, G. S. Bergreen, R. E. Davies, and M. Beck, Am. J. Phys. **72**, 1210 (2004)
5. P.G. Kwiat, E. Waks, A.G. White, I. Applebaum, and P.H. Eberhard, Phys. Rev. A **60**, 773 (1999).
6. M.J. Pysher, E.J. Galvez, K. Misra, K.R. Wilson, B.C. Melius, and M. Malik, Phys. Rev. A **72**, 052327 (2005).
7. D. Dehlinger and M. W. Mitchell, Am J. Phys. **70**, 903 (2003).